TRACER DIFFUSION IN COMPACTED, WATER-SATURATED BENTONITE

IAN C. BOURG[1,2,3,4,*], GARRISON SPOSITO[1,3] AND ALAIN C. M. BOURG[2]

[1] Civil and Environmental Engineering, Davis Hall # 1710, University of California, Berkeley, CA 94720-1710, USA
[2] Environmental HydroGeochemistry (LHGE-JE2397), Université de Pau et des Pays de l'Adour, BP 1155, 64013 Pau Cedex, France
[3] Geochemistry Department, Earth Sciences Division, Lawrence Berkeley National Laboratory, Berkeley, CA 94720, USA
[4] ANDRA, Parc de la Croix Blanche, 1/7 rue Jean Monnet, 92298 Châtenay-Malabry cedex, France

Abstract—Compacted Na-bentonite clay barriers, widely used in the isolation of solid-waste landfills and other contaminated sites, have been proposed for a similar use in the disposal of high-level radioactive waste. Molecular diffusion through the pore space in these barriers plays a key role in their performance, thus motivating recent measurements of the apparent diffusion coefficient tensor of water tracers in compacted, water-saturated Na-bentonites. In the present study, we introduce a conceptual model in which the pore space of water-saturated bentonite is divided into 'macropore' and 'interlayer nanopore' compartments. With this model we determine quantitatively the relative contributions of pore-network geometry (expressed as a geometric factor) and of the diffusive behavior of water molecules near montmorillonite basal surfaces (expressed as a constrictivity factor) to the apparent diffusion coefficient tensor. Our model predicts, in agreement with experiment, that the mean principal value of the apparent diffusion coefficient tensor follows a single relationship when plotted against the partial montmorillonite dry density (mass of montmorillonite per combined volume of montmorillonite and pore space). Using a single fitted parameter, the mean principal geometric factor, our model successfully describes this relationship for a broad range of bentonite-water systems, from dilute gel to highly-compacted bentonite with 80% of its pore water in interlayer nanopores.

Key Words—Bentonite, Diffusion, Geometric Factor, Interlayer, Montmorillonite, Nanopore, Smectite, Waste Containment.

INTRODUCTION

Sodium-bentonites (clays with high Na-montmorillonite content (Grim, 1968)) are used in engineered barriers and geosynthetic liners for the isolation of landfills and other contaminated sites (LaGrega *et al.*, 2001; Shackelford and Lee, 2003). These materials are also under consideration in several countries for use as barrier materials in the geological disposal of high-level radioactive waste (McCombie, 1997; JNC, 2000; ANDRA, 2001), where their low saturated hydraulic conductivity [$\sim 10^{-12}$ m s^{-1} (Madsen, 1998)] ensures that advective transport of radionuclides remains negligible in comparison to transport by molecular diffusion (Choi and Oscarson, 1996; JNC, 2000). Efforts to predict the performance of these barriers have motivated numerous experimental studies of the molecular diffusion of cations (Cs^+, Sr^{2+}, Na^+), anions (I^-, Cl^-, TcO_4^-) and water tracers (HDO, HTO) in compacted, water-saturated Na-bentonites (Torstenfelt, 1986; Muurinen *et al.*, 1987, 1989; Sato *et al.*, 1992; Kato *et al.*, 1995; Choi and Oscarson, 1996; Kozaki *et al.*, 1996, 1997, 1998, 1999; Eriksen *et al.*, 1999; Molera and Eriksen, 2002;

Liu *et al.*, 2003a, 2003b; Sato and Suzuki, 2003; Suzuki *et al.*, 2004).

In a water-saturated porous medium that is homogenous on the continuum scale, a macroscopic mass balance for a non-sorbing, conservative solute is derived from a Fickian expression with an apparent diffusion coefficient tensor $\mathbf{D_a}$ (with contributions from both hydrodynamic dispersion and molecular diffusion):

$$\frac{\partial C}{\partial t} = \nabla \cdot (\mathbf{D_a} \cdot \nabla C) - \mathbf{V} \cdot \nabla C \qquad (1)$$

where C is the concentration of the tracer in the pore solution and $\mathbf{V}$ is the Darcy velocity vector (Bear, 1972; Sposito *et al.*, 1979; Zheng and Bennett, 1995). In deriving equation 1, the solute mass flux density vector $\mathbf{N}$ is written (Sposito *et al.*, 1979):

$$\mathbf{N} = -\varepsilon \mathbf{D_a} \cdot \nabla C \qquad (2)$$

where ε is porosity (equal to the volumetric solution content of a water-saturated porous medium). If advection is negligible by comparison with molecular diffusion, the Darcy velocity term can be dropped from equation 1, and $\mathbf{D_a}$ can be taken as a diagonal tensor (Bear, 1972). Equations 1 and 2 then reduce to (Crank, 1975; Shackelford, 1991):

$$\frac{\partial C}{\partial t} = \frac{\partial}{\partial x_i}(D_{a,i}\frac{\partial C}{\partial x_i}) \qquad (3)$$

and

$$N_i = -\varepsilon D_{a,i}\frac{\partial C}{\partial x_i} \qquad (4)$$

where N_i and $D_{a,i}$ are the solute mass flux density and the apparent diffusion coefficient associated with the x_i (principal axis) direction.

Most models of tracer diffusion in compacted, water-saturated bentonite (Sato *et al.*, 1992; Lehikoinen *et al.*, 1999; Ochs *et al.*, 2001; Molera and Eriksen, 2002) simplify to an expression in which the relative apparent diffusion coefficient ($D_{a,i}/D_0$, with D_0 being the self-diffusion coefficient of the tracer in bulk liquid water) is determined by a geometric factor, $G_i \geqslant 1$, that describes the influence of pore-network geometry [*i.e.* the orientation, shape and connectivity of pores (Bear, 1972; Dykhuizen and Casey, 1989)]:

$$\frac{D_{a,i}}{D_0} = \frac{1}{G_i} \qquad (5)$$

Typical values of the geometric factor G_i for isotropic non-consolidated porous materials, determined by fitting equation 5 to experimental data, range from 1.2 to 3.0 (Satterfield *et al.*, 1973; van Brakel and Heertjes, 1974; Chantong and Massoth, 1983). For water tracers diffusing through compacted, water-saturated bentonite, values of G_i as high as 42 have been reported (Sato *et al.*, 1992).

Inherent in the use of equation 5 to interpret diffusion data is the assumption that only pore-network geometry affects the relative apparent diffusion coefficient of tracers (Bear, 1972; Dykhuizen and Casey, 1989). In porous media that contain a significant fraction of very small pores ('nanopores'), an additional parameter must be added to equation 5, the 'constrictivity factor' [$\delta \leqslant 1$ (Boving and Grathwohl, 2001)]:

$$\frac{D_{a,i}}{D_0} = \frac{\delta}{G_i} \qquad (6)$$

The term 'constrictivity' also has been used to describe a decrease in the apparent diffusion coefficient of tracers caused by pore-size variability (van Brakel and Heertjes, 1974). In equation 6, this contribution to the apparent diffusion coefficient is interpreted as caused by pore geometry, not by low water mobility near pore walls, so it is included in the geometric factor.

In compacted, water-saturated Na-bentonite, a fraction of the pore water is located in nanoscale interlayer pores between stacked montmorillonite lamellae (Kozaki

et al., 1998). For diffusion along a direction parallel to the pore walls, this interlayer water has a self-diffusion coefficient equal to ~60% of the self-diffusion coefficient of bulk water (Hall *et al.*, 1978; Chang *et al.*, 1995; Gay-Duchosal *et al.*, 2000; Marry and Turq, 2003). This reduction in the self-diffusion coefficient suggests that equation 6 should be used to describe the diffusion of water tracers (Kemper *et al.*, 1964; van Schaik *et al.*, 1966; Kato *et al.*, 1995). Long ago, Kemper *et al.* (1964) measured $D_{a,i}/D_0$ for HDO in films of oriented Na-montmorillonite lamellae formed by drying an aqueous suspension on a flat surface. They estimated the geometric factor to be equal to ~1.4 for diffusion along a direction parallel to the orientation of the lamellae, then determined δ from equation 6, finding it to vary from 0.3 to 1.0 over a range of water content corresponding to between one ($\delta = 0.3$) and 16 ($\delta \approx 1$) statistical monolayers of water molecules on each montmorillonite basal surface. Evidently δ reflects in some way the properties of water molecules that are vicinal to the basal surfaces bounding interlayers. Murad and Cushman (2000) have insisted that "a macroscopic model for smectic clays requires an accurate description of the anomalous behavior of the vicinal fluid. Hence, the treatment of the adsorbed water as a separate phase from the bulk water is mandatory". However, as pointed out recently by Michot *et al.* (2002), "the general problem of taking into account the specific behavior of vicinal water in transport phenomena in clay barriers remains largely unsolved".

On the other hand, a careful distinction between interlayer nanopores and larger pores ('macropores') has been applied successfully to explain the influence of water chemistry on the mechanics of clay swelling (Alonso and Navarro, 2002; Hueckel *et al.*, 2002). In the present article, we shall make the same distinction about the pore space to develop a new conceptual model of the diffusion of water tracers in compacted, water-saturated Na-bentonite using the physical context provided by equation 6. We shall substantiate the need for our model by a review of the evidence for nanopores in compacted, water-saturated bentonite and by a careful reanalysis of the available experimental data on $D_{a,i}$ for water tracers. Kato *et al.* (1995) and Suzuki *et al.* (2004) recently reported that $D_{a,i}$ in compacted bentonite is higher in a direction perpendicular ($D_{a,\perp}$) *vs.* parallel ($D_{a,\parallel}$) to the axis of compaction. Most published values of $D_{a,i}$ for water tracers in compacted, water-saturated bentonite are $D_{a,\parallel}$ values, which, if the results of Kato *et al.* (1995) and Suzuki *et al.* (2004) are of general validity, may underestimate $D_{a,i}$ for water tracers in an isotropically-compacted bentonite barrier. Furthermore, Liu *et al.* (2003a, 2003b) have shown that $D_{a,\parallel}$ for water tracers, as well as for Na and Sr ions, in mixtures of Na-montmorillonite and silica sand (39 to 72% montmorillonite by mass), when plotted as a function of the partial montmorillonite dry density ($\rho_{b,mont}$, the mass of

montmorillonite per combined volume of montmorillonite and pore space, calculated as in Bourg, 2004), were not significantly different from values of $D_{a,\parallel}$ obtained with the same diffusing species in pure Na-montmorillonite. This very interesting finding suggests that experimental data obtained with different bentonites may be reducible to a single relation between $D_{a,i}/D_0$ and the 'master variable' $\rho_{b,mont}$. Accordingly, our conceptual model development will be based on a careful re-examination of the available database for $D_{a,i}$ obtained using water tracers.

NANOPORES IN COMPACTED, WATER-SATURATED BENTONITE

To facilitate the interpretation of water-tracer diffusion experiments, bentonite-water mixtures will be classified as bentonite suspensions if $\rho_{b,mont} < 0.1-0.2$ kg dm^{-3}, bentonite gels for $0.1-0.2$ kg dm$^{-3} < \rho_{b,mont} < 0.8-1.0$ kg dm^{-3}, and compacted bentonite if $\rho_{b,mont} > 0.8-1.0$ kg dm^{-3}. The term 'suspension' distinguishes bentonite systems in which particles comprising individual lamellae or stacks of a few lamellae move relatively freely in an aqueous solution (Sposito, 1992) from 'gels' in which these particles are linked in a bulky turbostratic fashion often termed a 'house-of-cards' structure (Güven, 1992). Prior to diffusion experiments to be carried out at $\rho_{b,mont} > 0.8-1.0$ kg dm^{-3}, a bentonite sample is first compacted in an air-dried or oven-dried state to a lower volume than that occupied by the dry powder, then saturated with water while being maintained at constant volume. The limited amount of swelling allowed under these conditions causes the compacted bentonite to retain some of the microstructure of dry bentonite. Thus, on the length scale of tens of micrometers, the fabric of the dry material (with aggregates of Na-montmorillonite separated by large pores) is partly preserved after hydration, yielding microscale regions of high and low bulk density (Pusch, 1999; Kozaki et al., 2001b; Liu et al., 2003b).

On the length scale of hundreds to thousands of nanometers, scanning electron microscopy (SEM) reveals that uniaxial compaction can cause an orientation of the layers of clay lamellae in a direction normal to that of compaction, a tendency that increases with the dry bulk density (Sato and Suzuki, 2003). Sato and Suzuki (2003) observed such a preferential orientation of the montmorillonite lamellae in compacted Kunipia-F bentonite (99% Na-montmorillonite) at $\rho_{b,mont} = 0.98$, 1.56 and 1.95 kg dm^{-3}, but could not detect it in Kunigel-V1 bentonite (46−49% Na-montmorillonite) at $\rho_{b,mont} = 0.57$, 1.05 and 1.47 kg dm^{-3}. These results suggest that grains of impurities (i.e. non-montmorillonitic solids) may prevent stacks of montmorillonite lamellae from orienting themselves normal to the direction of compaction.

On the length scale of tens of nanometers, the parallel stacking of montmorillonite lamellae present in dry

bentonite is partly preserved after the hydration of compacted bentonite, as proven by the existence of X-ray diffraction (XRD) peaks at dry bulk densities of 1.0 kg dm^{-3} or more ($\rho_{b,mont} \geqslant 0.98$ kg dm^{-3}) in compacted, water-saturated Na-montmorillonite (Kozaki et al., 1998, 2001a). Kozaki et al. (1998, 2001a) observed a 3-layer hydrate of Na-montmorillonite (basal spacing of 1.80 to 1.87 nm) from 1.0 to 1.5 kg dm^{-3} dry bulk density ($\rho_{b,mont} = 0.98$ to 1.47 kg dm^{-3}), and a 2-layer hydrate (basal spacing of 1.53 to 1.57 nm) from 1.4 to 1.8 kg dm^{-3} dry bulk density ($\rho_{b,mont} = 1.37$ to 1.76 kg dm^{-3}). Kozaki et al. (2001a) calculated the fraction of interlayer water in the compacted clay ($f_{interlayer}$) from the equation:

$$f_{interlayer} = \frac{a_{s,internal} \, d_{interlayer}}{2} \frac{\rho_w}{m_w} \qquad (7)$$

where $a_{s,internal}$ is the internal specific surface area (the specific area of the basal surfaces bounding the interlayers), $d_{interlayer}$ is the interlayer thickness, ρ_w is the mass density of liquid water, and m_w is the gravimetric water content of the compacted bentonite. Kozaki et al. (2001a) estimated $d_{interlayer}$ from their XRD results (Figure 1), measured m_w as the weight loss of

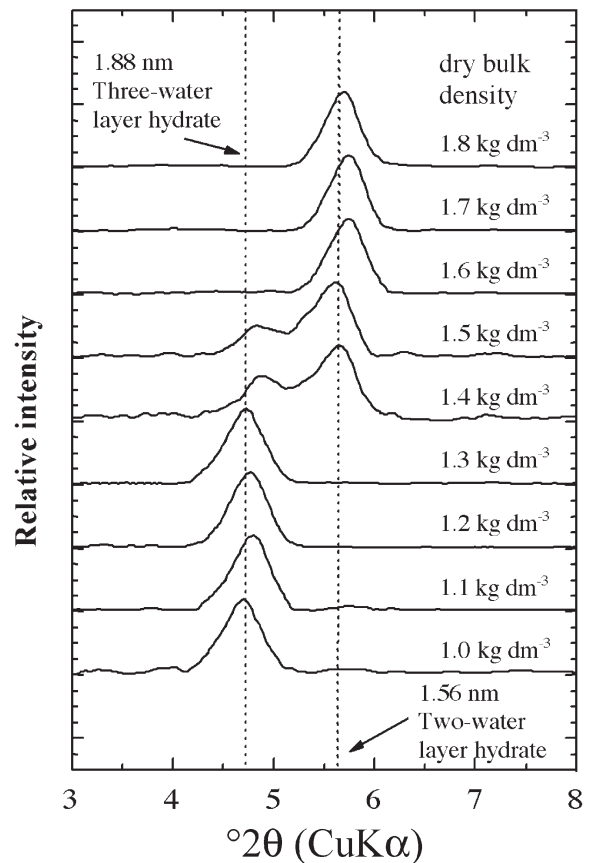Figure 1. XRD patterns (CuKα radiation) for compacted, water-saturated Na-montmorillonite at several values of dry bulk density (Kozaki et al., 1998).

water-saturated bentonite upon drying to 378 K, and calculated $a_{s,internal}$ from the relationship:

$$a_{s,internal} = a_s - a_{s,external} \qquad (8)$$

where a_s (the total specific surface area) was determined by adsorption of EGME (ethylene glycol monoethyl ether), and $a_{s,external}$ (the specific surface area of the external surfaces of stacked lamalllae) was determined by N_2 adsorption. Using equations 7 and 8 with their data, Kozaki *et al.* (2001a) found the important result that only interlayer water remained in compacted, water-saturated bentonite at $\rho_{b,mont} > 1.75$ kg dm^{-3}.

These studies indicate that compacted, water-saturated Na-bentonite ($\rho_{b,mont} > 0.8-1.0$ kg dm^{-3}) contains both nanoscale interlayer pores — nanopores — and larger intra- or inter-aggregate pores — macropores. The interlayer porosity is not negligible, and its contribution to the total porosity increases with the partial montmorillonite dry density until only interlayer pores are present for $\rho_{b,mont} > 1.75$ kg dm^{-3}. Aggregate structure is not entirely dispersed upon hydration of compacted bentonite, however, causing microscale regions of relatively high or low partial montmorillonite dry density (*i.e.* regions with either more nanopores or more macropores) to coexist within the same sample. The stacking of montmorillonite lamellae is preserved in compacted bentonite, although the average stack size may change as the clay is hydrated. One-dimensional compaction causes the montmorillonite lamellae (or stacks of lamellae) to orient preferentially in a direction normal to that of sample compaction, a behavior that may be disrupted by the presence of non-montmorillonitic solids.

APPARENT DIFFUSION COEFFICIENTS OF WATER TRACERS

We have compiled experimental values of the relative apparent diffusion coefficient ($D_{a,i}/D_0$) of water tracers in saturated Kunipia-F and Kunigel-V1 bentonites at 298 K (Figures 2 and 3). (Details of the experimental methods used to obtain the data reported in Figures 2 and 3, as well as methods of calculation for the error bars (95% confidence intervals) in the figures and for all other confidence intervals reported in this paper, can be found in Bourg, 2004). These two bentonites contain 99% and 46−49% montmorillonite, respectively, with Na$^+$ as the main exchangeable cation (Nakazawa *et al.*, 1999; Sato and Suzuki, 2003). In Figure 2, we have included values of $D_{a,i}/D_0$ obtained with Na-montmorillonite (purified Kunipia-F bentonite (Kozaki *et al.*, 1999)) and with mixtures of Na-montmorillonite and silica sand (Liu *et al.*, 2003a). The data are plotted as a function of $\rho_{b,mont}$, calculated as in Bourg (2004).

The relative apparent diffusion coefficients shown in Figures 2 and 3 were calculated from the measured apparent diffusion coefficients ($D_{a,i}$) and from the tracer diffusion coefficient of water isotopes in pure liquid water at 298 K [$D_0 = 2.30$, 2.27 and 2.24×10^{-9} m^2 s^{-1}, respectively, for H$_2$O, HDO and HTO in H$_2$O at 298 K (Mills, 1973)]. The values of $D_{a,i}$ used to construct Figures 2 and 3 were measured at 298 K, except for those of Nakazawa *et al.* (1999), obtained at 303 K, those of Nakashima (2000), obtained at 303.5 K, and those of Sato *et al.* (1992) and Kato *et al.* (1995), obtained at "room temperature", which we assumed equal to 288±5 K. (The confidence interval for the
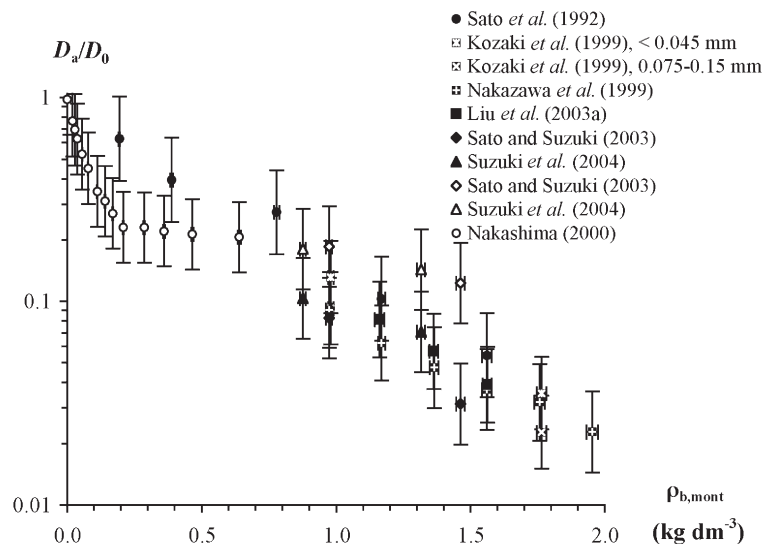

Figure 2. Logarithm of the relative apparent diffusion coefficient of water tracers at 298 K (calculated using $D_0 = 2.30$, 2.27 and 2.24×10^{-9} m^2 s^{-1} for H$_2$O, HDO and HTO (Mills, 1973)) in compacted Kunipia-F bentonite, Na-montmorillonite or Na-montmorillonite/sand mixtures (39−72% montmorillonite, Liu *et al.*, 2003a) plotted against the partial montmorillonite dry density. Filled non-circular symbols: measured parallel to compaction ($D_{a,\parallel}$). Open non-circular symbols: measured normal to compaction ($D_{a,\perp}$). ○: NMR method.

temperature at which experiments were performed was included in estimates of the confidence interval of $D_{a,i}$, as described in Bourg, 2004.) We extrapolated these results to 298 K, using the activation energy of the apparent diffusion coefficient ($E_{A,a}$), measured by Nakazawa *et al.* (1999) and Nakashima (2000), assuming an Arrhenius relation between the apparent diffusion coefficient and temperature (Calvet, 1973; Nakashima, 2000):

$$D_{a,i} = Be^{-\frac{E_{A,a}}{RT}} \qquad (9)$$

where $D_{a,i}$ is the apparent diffusion coefficient at absolute temperature T, B is an exponential pre-factor with units of $m^2\ s^{-1}$, and R is the molar gas constant ($8.314\ J\ mol^{-1}\ K^{-1}$).

The data near $\rho_{b,mont}$ = 1.5 kg dm^{-3} for Kunipia-F bentonite (Figure 2) confirm the conclusion of Sato and Suzuki (2003), that one-dimensional compaction to high values of $\rho_{b,mont}$ can cause some anisotropy in the apparent diffusion coefficient tensor ($D_{a,\perp} > D_{a,\parallel}$). To reveal effects on D_a other than those caused by compaction anisotropy, we have calculated the mean principal value of the apparent diffusion coefficient tensor (mean principal apparent diffusion coefficient, D_a), assuming it to be axially symmetric, using data on apparent diffusion coefficients measured in directions parallel and normal to compaction along with the standard equation:

$$D_a = \frac{D_{a,\parallel} + 2D_{a,\perp}}{3} \qquad (10)$$

Measurements by pulsed-field gradient nuclear magnetic resonance (PFG NMR) spectroscopy (Nakashima, 2000, 2004) directly yield D_a, as they probe the displacement of "tagged" water molecules in all directions over time-scales on the order of 10^{-2} to 10^0 s, so we have included data obtained by this method in Figure 4.

As is evident in Figure 4, the relationship between mean principal apparent diffusion coefficient and partial montmorillonite dry density is not significantly different for the Kunigel-V1 and Kunipia-F bentonites. Plotted in this way, the data seem to follow a single curve, within experimental precision. Thus we confirm the conclusion of Liu *et al.* (2003a), who judged the apparent diffusion coefficient ($D_{a,\parallel}$) of HTO in montmorillonite/sand mixtures to be similar to that determined by Nakazawa *et al.* (1999) and Kozaki *et al.* (1999) in pure montmorillonite at the same partial montmorillonite dry density.

ESTIMATION OF THE GEOMETRIC AND CONSTRICTIVITY FACTORS

The geometric and constrictivity factors for water tracers in bentonite appear to have been measured in only two studies (Kemper *et al.*, 1964; Nakashima, 2002). Kemper *et al.* (1964), as mentioned in the Introduction, determined the apparent diffusion coefficient of a HDO tracer in samples of oriented montmorillonite lamellae formed by drying a suspension of montmorillonite on a flat surface. Water diffusion was measured in a direction parallel to the orientation of the lamellae, for which the geometric factor was estimated
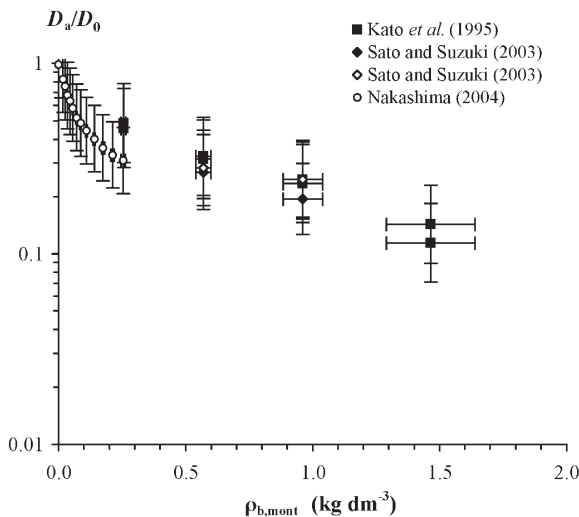

Figure 3. Logarithm of the relative apparent diffusion coefficient of water tracers at 298 K in compacted Kunigel-V1 bentonite (46–49% montmorillonite) plotted against the partial montmorillonite dry density. Filled non-circular symbols: $D_{a,\parallel}$. Open non-circular symbols: $D_{a,\perp}$. ○: NMR method.
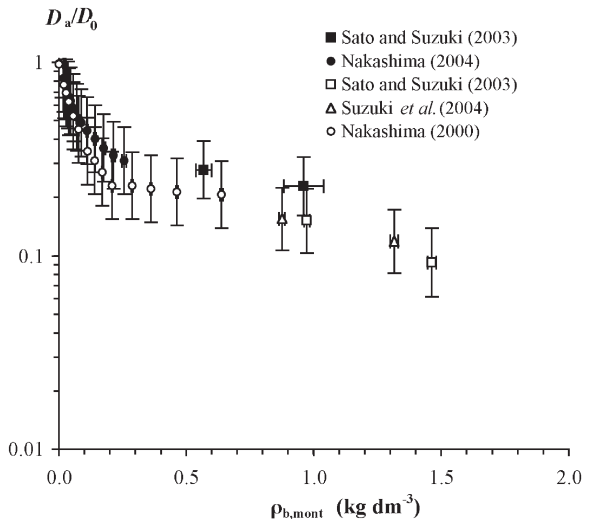
Figure 4. Logarithm of the relative mean principal apparent diffusion coefficient of water tracers at 298 K in compacted bentonite (filled symbols: Kunigel-V1; open symbols: Kunipia-F and Na-montmorillonite) plotted against the partial montmorillonite dry density.

as equal to ~1.4. At the lowest water content studied (one statistical monolayer of water molecules on each surface, *i.e.* a 2-layer hydrate), Kemper *et al.* (1964) found $D_{a,i}/D_0 = 0.2$. From equation 6, they concluded that the average mobility of HDO in the 2-layer hydrate of montmorillonite was only ~30% of the mobility in bulk water (*i.e.* δ = 0.3).

Nakashima (2002) compared the apparent diffusion coefficients of water tracers and I^- in Na-bentonite suspensions and gels, suggesting that the two diffusing species were equally affected by the geometric factor, but that I^-, because of anion exclusion from the basal surfaces of negatively-charged montmorillonite lamellae, was not affected by the low mobility of water near these surfaces (*i.e.* δ = 1 for I^-). The relative apparent diffusion coefficient of water tracers measured by Nakashima (2002) was only slightly lower than that of I^- at dry bulk densities of 0 to 0.2 kg dm^{-3}, from which Nakashima (2002) concluded that the fourfold decrease in D_a/D_0 observed in this range of dry bulk density was caused mainly by a concomitant increase in the geometric factor.

Based on these measurements of the geometric and constrictivity factors in Na-montmorillonite, an interpretation of the trend in D_a/D_0 *vs.* $\rho_{b,mont}$ (Figure 4) can be proposed. The dominant contribution of a changing geometric factor is indicated by gray symbols in Figure 5 (where experimental data obtained with Kunigel-V1 bentonite are omitted for the sake of clarity). The interpretation of these data is that, had it not been decreased by the lower mobility of water near montmorillonite surfaces, the relative apparent diffusion coefficient of water tracers would have been equal to that for I^-. Thus the mean principal geometric factor for water tracers, G, can be calculated directly from the I^-

data: $(D_a/D_0)_{I^-} = 1/G = 0.32\pm0.13$ at $\rho_{b,mont} = 0.2$ kg dm^{-3}. Extrapolating linearly the values of log (D_a/D_0) obtained for $\rho_{b,mont}$ between 0.9 and 1.5 kg dm^{-3}, we estimate $D_a/D_0 = 0.08\pm0.04$ at $\rho_{b,mont} = 1.75$ kg dm^{-3}, to which we have assigned a confidence interval ~50% larger than that of the experimental data themselves (Figure 5). At this value of $\rho_{b,mont}$, most of the pore space of compacted, water-saturated bentonite is in the 2-layer hydrate (Kozaki *et al.*, 1998). Introducing the extrapolated D_a/D_0 along with the result of Kemper *et al.* (1964) for the constrictivity factor in the 2-layer hydrate of Na-montmorillonite (δ = 0.3) into equation 6, we can estimate the value of D_a/D_0 that would have been measured at $\rho_{b,mont} = 1.75$ kg dm^{-3} if diffusion through the 2-layer hydrate were not slowed in the vicinity of the basal surface. This estimate, $D_a/D_0 \equiv 1/G = 0.27\pm0.13$, is also shown in Figure 5. We can conclude accordingly that, although the geometric factor increases approximately fourfold between $\rho_{b,mont} \approx 0$ kg dm^{-3} (pure liquid water) and 0.2 kg dm^{-3} (concentrated suspension or dilute gel), it varies negligibly, within experimental precision, over the range of partial montmorillonite densities above 0.2 kg dm^{-3}, *i.e.* for concentrated gels and compacted bentonites.

The rapid increase in the geometric factor for $\rho_{b,mont}$ <0.2 kg dm^{-3}, and the subsequent constant value (within experimental precision) of the mean principal geometric factor at higher partial montmorillonite dry densities, can be interpreted as follows. In pure water, $G = 1$, but in the presence of montmorillonite particles, diffusion paths in the vicinity of the particles are forced to be parallel with their basal surfaces (ignoring the very small edge surface area of the particles). As $\rho_{b,mont}$ increases, the fraction of the water volume in which diffusion paths are randomly oriented, as they are in the
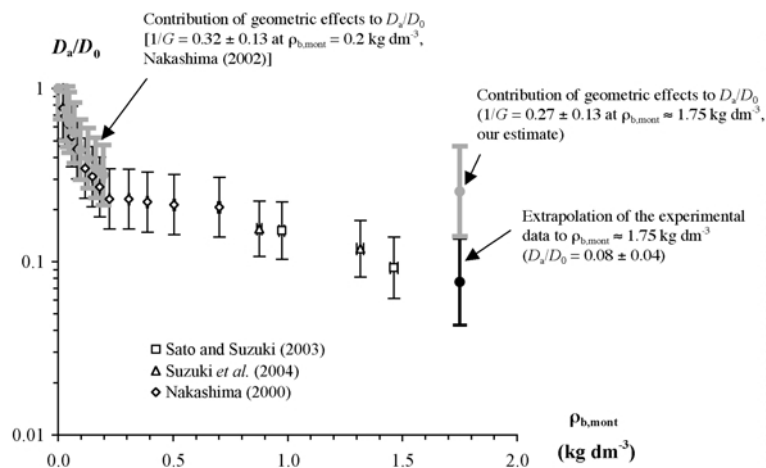

Figure 5. Logarithm of the mean principal value of the relative apparent diffusion coefficient of water tracers in Kunipia-F bentonite and Na-montmorillonite at 298 K. Experimental data from Figure 4 (open non-circular symbols) and extrapolation to $\rho_{b,mont} = 1.75$ kg dm^{-3} (black, filled non-circular symbol) plotted against the partial montmorillonite dry density. Gray symbols are estimates of the contribution of geometric effects to D_a/D_0 based on data from Nakashima (2002) at $\rho_{b,mont} = 0$ to 0.2 kg dm^{-3} and from the present study at $\rho_{b,mont} = 1.75$ kg dm^{-3}.

bulk liquid, progressively decreases, and the fraction of the volume of water in which diffusion paths are forced to be parallel with the basal surfaces increases, causing an increase in the geometric factor. The observation that the geometric factor does not change significantly for $\rho_{b,mont} > 0.2$ kg dm^{-3} suggests that, above this value of $\rho_{b,mont}$, all tracer diffusion paths are affected to some extent by the montmorillonite basal surfaces. At $\rho_{b,mont} = 0.2$ kg dm^{-3}, the average thickness of water layers on the basal surfaces is 6 nm, which is much less than the lateral extent of a typical montmorillonite particle [~500 nm (Güven, 1992)]. Within this thin water layer, diffusion paths would be expected to be approximately parallel to the basal surface. Further increases in $\rho_{b,mont}$ cause a decrease in the volume of macropores relative to interlayer nanopores, but diffusion paths still remain parallel, or nearly parallel, to the vicinal basal surfaces − even if the montmorillonite lamellae themselves are isotropically oriented − and the geometric factor should not be affected by compaction above $\rho_{b,mont} \approx 0.2$ kg dm^{-3}, as indicated by the data in Figure 5.

MODEL OF THE APPARENT DIFFUSION COEFFICIENT

Model development

We shall conceptually divide the pore space of compacted, water-saturated bentonite into interlayer nanopore and macropore categories. A representative elementary volume of the bentonite is composed of three compartments: the solid phase, macropores, and interlayer nanopores, which occupy the volume fractions ε_{solid}, $\varepsilon_{macropore}$ and $\varepsilon_{interlayer}$, respectively. Therefore, the porosity partitions according to the relation:

$$\varepsilon = \varepsilon_{macropore} + \varepsilon_{interlayer} \qquad (11)$$

We propose further to describe diffusion through the macropore and nanopore compartments as independent, parallel processes with distinct values of D_a/D_0 ($(D_a/D_0)_{macropore}$ and $(D_a/D_0)_{interlayer}$), and to model the relative apparent diffusion coefficient of tracers in compacted, water-saturated bentonite as the weighted average of D_a/D_0 in the macropore and nanopore compartments, with weighting by the mole fractions of pore water in each compartment, which are closely approximated by the respective volume fractions, $\varepsilon_{macropore}/\varepsilon$ and $\varepsilon_{interlayer}/\varepsilon$. If we use equation 6 to represent $(D_a/D_0)_{macropore}$ and $(D_a/D_0)_{interlayer}$, we obtain the model expression:

$$\frac{D_a}{D_0} = \frac{\delta_{macropore}}{G_{macropore}}\frac{\varepsilon_{macropore}}{\varepsilon} + \frac{\delta_{interlayer}}{G_{interlayer}}\frac{\varepsilon_{interlayer}}{\varepsilon} \qquad (12)$$

If we now define $f_{interlayer}$ as the volume fraction of interlayer nanopores, a generalization of equation 7,

$$f_{interlayer} = \frac{\varepsilon_{interlayer}}{\varepsilon} \qquad (13)$$

we obtain, combining equations 12 and 13:

$$\frac{D_a}{D_0} = \frac{\delta_{macropore}}{G_{macropore}}\left(1 - f_{interlayer}\right) + \frac{\delta_{interlayer}}{G_{interlayer}}f_{interlayer} \qquad (14)$$

By definition, $\delta_{macropore} \approx 1$, because macropores, of the order of tens of nanometers to micrometers in diameter (Choi and Oscarson, 1996), are much larger than the diameter of a water molecule, 0.29 nm. Furthermore, the geometric factor is not significantly different at $\rho_{b,mont} = 1.75$ kg dm^{-3} (when most pores are nanopores) from its value at $\rho_{b,mont} = 0.2$ kg dm^{-3} (when most pores are macropores). Therefore $G_{macropore} \approx G_{interlayer} \approx G$. Applying these simplifications to equation 14, we obtain a model expression for D_a/D_0 in compacted, water-saturated bentonite:

$$\frac{D_a}{D_0} = \frac{1}{G}\left[\left(1 - f_{interlayer}\right) + \delta_{interlayer}f_{interlayer}\right] \qquad (15)$$

where, based on the results of Kemper et al. (1964), $\delta_{interlayer} = 0.30 \pm 0.05$. We assume that the value of $\delta_{interlayer}$ is not significantly affected by compaction going from the 3- to the 2-layer hydrate. Molecular dynamics simulations predict similar self-diffusion coefficients in interlayer pores for water in 2- and 3-layer hydrates (Chang et al., 1995). Semi-empirical equations based on studies of membrane filtration yield statistically similar values of $\delta_{interlayer}$ for water in the 2- and 3-layer montmorillonite hydrates (Bourg, 2004), with both values consistent with the experimental data of Kemper et al. (1964). Thus only $f_{interlayer}$ and G must be estimated in order to predict D_a/D_0.

Estimating $f_{interlayer}$

Limiting ourselves to partial montmorillonite dry densities at which the 1-layer hydrate is not present, i.e. $\rho_{b,mont} < 1.75$ kg dm^{-3} (Kozaki et al., 1998), we can write, with $\varepsilon_{2-layer}$ and $\varepsilon_{3-layer}$ being the volume fractions of the 2- and 3-layer hydrates,

$$\varepsilon_{interlayer} = \varepsilon_{2-layer} + \varepsilon_{3-layer} \qquad (16)$$

and further define $\xi_{2-layer}$ as the volume fraction of the 2-layer hydrate in the nanopores:

$$\xi_{2-layer} = \frac{\varepsilon_{2-layer}}{\varepsilon_{interlayer}} \qquad (17)$$

If ε_{imp} is the volume fraction occupied by impurities (i.e. non-montmorillonitic solids) in compacted bentonite, and ρ_{mont} is the mass density of a montmorillonite lamella, we can factorize the porosity as:

$$\varepsilon = \left(1 - \varepsilon_{imp}\right)\left(1 - \frac{\rho_{b,mont}}{\rho_{mont}}\right) \qquad (18)$$

where $(1 - \rho_{b,mont}/\rho_{mont})$ is the volume fraction of pores in an element of volume not occupied by impurities and $(1 - \varepsilon_{imp})$ is its corresponding volume fraction in the entire system. The volume fraction occupied by the 2-layer hydrate $(\varepsilon_{2\text{-layer}})$ can be calculated from the volume fraction of the 2-layer hydrate in interlayer nanopores $(\xi_{2\text{-layer}})$, the thickness of water layers present in the nanopores of the 2- and 3-layer hydrates $(d_{2\text{-layer}}$ and $d_{3\text{-layer}})$, and the specific surface area of montmorillonite basal surfaces $(a_{s,internal})$:

$$\varepsilon_{2\text{-layer}} =$$

$$\left(1 - \varepsilon_{imp}\right)\rho_{b,mont}a_{s,internal}\frac{d_{2\text{-layer}}}{2}\left\{\frac{\dfrac{\xi_{2\text{-layer}}}{d_{2\text{-layer}}}}{\dfrac{\xi_{2\text{-layer}}}{d_{2\text{-layer}}}+\dfrac{1-\xi_{2\text{-layer}}}{d_{3\text{-layer}}}}\right\} \qquad (19)$$

Interlayer water in the 2-layer hydrate is described in equation 19 as a statistical water layer of thickness $d_{2\text{-layer}}/2$, weighted by the term in brackets, which is the number fraction of interlayer nanopores that are 2-layer hydrates. We can express the volume fraction occupied by the 3-layer hydrate in the same way:

$$\varepsilon_{3\text{-layer}} =$$

$$\left(1 - \varepsilon_{imp}\right)\rho_{b,mont}a_{s,internal}\frac{d_{3\text{-layer}}}{2}\left\{\frac{\dfrac{1-\xi_{2\text{-layer}}}{d_{3\text{-layer}}}}{\dfrac{\xi_{2\text{-layer}}}{d_{2\text{-layer}}}+\dfrac{1-\xi_{2\text{-layer}}}{d_{3\text{-layer}}}}\right\} \qquad (20)$$

Equations 13, 16 and 18–20 are then combined to yield the following model expression for $f_{interlayer}$:

$$f_{interlayer} =$$

$$\frac{1}{2}a_{s,internal}\frac{\rho_{mont}\rho_{b,mont}}{\rho_{mont}-\rho_{b,mont}}\frac{1}{\dfrac{\xi_{2\text{-layer}}}{d_{2\text{-layer}}}+\dfrac{1-\xi_{2\text{-layer}}}{d_{3\text{-layer}}}} \qquad (21)$$

Equation 21 reduces to equation 7 if only one type of hydrate is present and there are no solid-phase impurities. All of the predicted dependence of D_a/D_0 on $\rho_{b,mont}$ is contained in $f_{interlayer}$.

The specific volume of montmorillonite lamellae (the inverse of the mass density of a lamella) can be expressed as the product of the thickness of a lamella (d_{mont}) by half its basal plane specific surface area:

$$\frac{1}{\rho_{mont}} = \frac{d_{mont}a_{s,internal}}{2} \qquad (22)$$

Finally, combining equations 21 and 22, we obtain an expression describing $f_{interlayer}$ as a function of the thickness and mass density of montmorillonite lamellae $(d_{mont}$ and $\rho_{mont})$, $\rho_{b,mont}$, the thickness of the 2- and 3-layer hydrates $(d_{2\text{-layer}}$ and $d_{3\text{-layer}})$, and the volume fraction of the 2-layer hydrate in the interlayers $(\xi_{2\text{-layer}})$:

$$f_{interlayer} =$$

$$\frac{1}{d_{mont}}\frac{\rho_{b,mont}}{\rho_{mont}-\rho_{b,mont}}\frac{1}{\dfrac{\xi_{2\text{-layer}}}{d_{2\text{-layer}}}+\dfrac{1-\xi_{2\text{-layer}}}{d_{3\text{-layer}}}} \qquad (23)$$

In equation 23, the $d_{mont} = (d_{basal} - d_{interlayer})$, where d_{basal} is a basal spacing of a montmorillonite hydrate as measured by XRD and $d_{interlayer}$ is the statistical thickness of water in its interlayers (equal to $d_{2\text{-layer}}$ and $d_{3\text{-layer}}$, respectively, in the 2- and 3-layer hydrates). From their Monte Carlo simulations of interlayer water, Chang *et al.* (1995) reported basal spacings of 15.28 ± 0.06 and 18.77 ± 0.06 Å in the 2- and 3-layer hydrates of Na-montmorillonite, respectively, and provided computed interlayer water molecule density from which we calculated a thickness of interlayer water equal to 5.91 and 9.35 Å in the 2- and 3-layer hydrates. From these values of d_{basal} and $d_{interlayer}$, we obtain $d_{mont} = 9.4\pm0.1$ Å for the 2- and 3-layer hydrates, which we used in equation 23. The smallest basal spacing measured for montmorillonite is 9.4 Å (Bérend *et al.*, 1995). The basal spacing of dry Na-montmorillonite is 9.55–9.60 Å (Calvet, 1973; Keren and Shainberg, 1975; Bérend *et al.*, 1995), probably because Na^+ counterions tend to open the interlayers slightly (Pezerat and Méring, 1967).

A mass density (ρ_{mont}) of 2.88 kg dm^{-3} has been measured by Suzuki *et al.* (2004) for the montmorillonite in Kunipia-F bentonite, and mass densities of 2.80 and 2.83 kg dm^{-3} have been measured for other montmorillonites by Low and Anderson (1958) and Bradley (1959).

The mass density of montmorillonite lamellae can also be calculated from the a,b dimensions and chemical formula of a unit-cell. If FW is the formula mass per unit-cell, a and b the dimensions of the cell in a basal plane, and N_A is the Avogadro constant (6.022×10^{23} mol^{-1}), then:

$$\rho_{mont} = \frac{FW}{abd_{mont}N_A} \qquad (24)$$

Using $FW = 746\pm1$ g mol^{-1} and $ab = 46.4\pm0.4$ Å^2 (Bourg, 2004), we obtain $\rho_{mont} = 2.84\pm0.04$ kg dm^{-3}, which agrees with the measured values.

Basal spacings measured for Na-montmorillonite range from 15.3 to 15.7 Å for the 2-layer hydrate, and from 18.0 to 18.9 Å for the 3-layer hydrate (Calvet, 1973; Keren and Shainberg, 1975; Watanabe and Sato, 1988; Cases *et al.*, 1992; Bérend *et al.*, 1995). By subtracting the thickness of a montmorillonite lamella (d_{mont} = 9.4±0.1 Å) from these basal spacings, we obtain interlayer spacings $d_{2-layer}$ = 6.1±0.2 Å and $d_{3-layer}$ = 9.0±0.5 Å (the thickness of two and three layers of water molecules), respectively, in the 2- and 3-layer hydrates.

We can estimate the volume fraction of the 2-layer hydrate in the interlayer pores ($\xi_{2-layer}$) from the XRD results obtained by Kozaki *et al.* (1998, 2001a) for water-saturated Na-montmorillonite at $0.98 < \rho_{b,mont} < 1.76$ kg dm^{-3} (Figure 1). The XRD results show only the 3-layer hydrate ($\xi_{2-layer}$ = 0) for $0.98 \leqslant \rho_{b,mont} \leqslant 1.27$ kg dm^{-3} and only the 2-layer hydrate ($\xi_{2-layer}$ = 1) for $1.57 \leqslant \rho_{b,mont} \leqslant 1.76$ kg dm^{-3}. At $\rho_{b,mont}$ = 1.37 and 1.47 kg dm^{-3}, the results indicated the presence of both the 2- and 3-layer hydrates. In equation 23, we have decided to represent $\xi_{2-layer}$ as a 'ramp' function, increasing linearly (and with linearly increasing uncertainty) from $\xi_{2-layer}$ = 0.0 at $\rho_{b,mont}$ = 1.27 kg dm^{-3} to $\xi_{2-layer}$ = 0.5 ± 0.5 at $\rho_{b,mont}$ = 1.42 kg dm^{-3}, then increasing linearly (with a linearly decreasing uncertainty) to $\xi_{2-layer}$ = 1.0 at $\rho_{b,mont}$ = 1.57 kg dm^{-3}.

Values of $f_{interlayer}$ corresponding to incremented values of $\rho_{b,mont}$ as obtained with the parameter values given in the present section are reported in Table 1. These model results immediately confirm the conclusion of Kozaki *et al.* (2001a), that only interlayer nanopores

are present in compacted, water-saturated Na-bentonite at $\rho_{b,mont}$ = 1.75 kg dm^{-3} (to be more precise, $\rho_{b,mont}$ = 1.72 ± 0.04 kg dm^{-3}, according to equation 23).

Estimating G

Kato *et al.* (1995) and Ichikawa *et al.* (2004) have recommended G = 3, the geometric factor of an isotropic, well-connected network of straight cylindrical pores (Bear, 1972; Dykhuizen and Casey, 1989), for compacted, water-saturated bentonite. Although the use of G = 3 in equation 15 yields a good description of experimental data on D_a/D_0 in Kunigel-V1 bentonite, it appears to overestimate the data obtained for Kunipia-F bentonite (non-circular open symbols in Figure 6). Alternatively, equation 15 and experimental values of the mean principal apparent diffusion coefficient (Figure 4) can be combined to fit the value of G for compacted, water-saturated bentonite, as follows:

$$G = \frac{D_0}{D_a}\left[\left(1 - f_{interlayer}\right) + \delta_{interlayer}f_{interlayer}\right] \qquad (25)$$

Inserting the four available values of (D_a/D_0) for water tracers at $\rho_{b,mont} \geqslant 0.96$ kg dm^{-3} into equation 25, we obtain G = 4.0 ± 1.6 (the 95% confidence interval is the average of the confidence intervals on four estimates of G). The relative apparent diffusion coefficient of water tracers calculated from equation 15 with the fitted G value is compared to experimental data in Figure 7.

Equation 15 and Table 1 with δ = 0.3 ± 0.05 and G = 4.0 ± 1.6 describe the experimental data well for $\rho_{b,mont}$
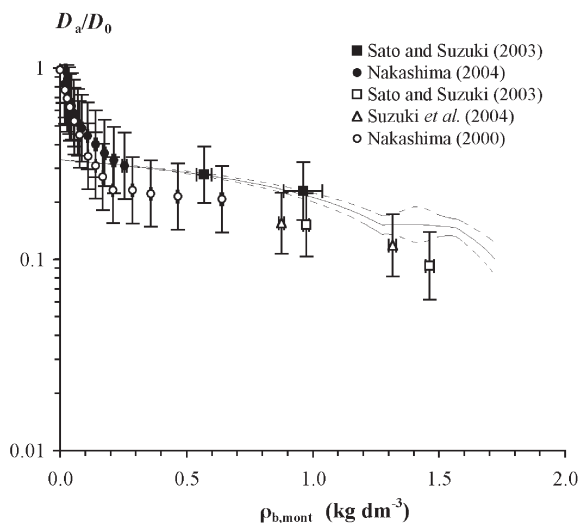

Figure 6. Logarithm of the relative mean principal apparent diffusion coefficient of water tracers in Na-bentonite (experimental data from Figure 4) plotted against the partial montmorillonite dry density. Closed symbols: Kunigel-V1. Open symbols: Kunipia-F and Na-montmorillonite. Solid curve is the relative apparent diffusion coefficient calculated from equation 15 using G = 3, with its upper and lower 95% confidence interval shown as dashed curves.
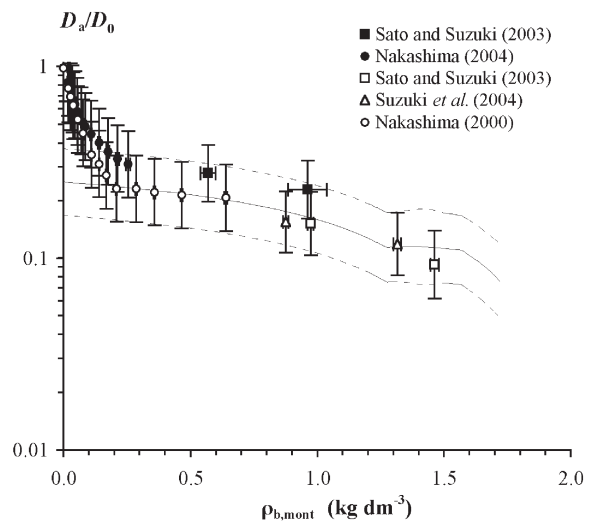
Figure 7. Logarithm of the relative mean principal apparent diffusion coefficient of water tracers in Na-bentonite (experimental data from Figure 4) plotted against the partial montmorillonite dry density. Closed symbols: Kunigel-V1. Open symbols: Kunipia-F and Na-montmorillonite. Solid curve is the relative apparent diffusion coefficient calculated from equation 15 using G = 4.0±1.6, with its upper and lower 95% confidence interval shown as dashed curves.

Table 1. Model prediction of the volume fraction of interlayer nanopores in water-saturated Na-bentonite ($f_{interlayer}$) as a function of partial montmorillonite dry density (equation 23).

$\rho_{b,mont}$ (kg dm^{-3})	$f_{interlayer}$
1.0	0.52±0.03
1.1	0.61±0.04
1.2	0.70±0.04
1.3	0.78±0.05
1.4	0.77±0.14
1.5	0.78±0.07
1.6	0.84±0.04
1.7	0.96±0.04

> 0.2 kg dm^{-3}, although the assumption that most of the water affected by the bentonite surface is located in 2- or 3-layer hydrates is strictly valid only for $0.98 < \rho_{b,mont} < 1.72$ kg dm^{-3}. The model prediction, constructed using a single adjustable parameter ($G = 4.0 \pm 1.6$), successfully describes the relative mean principal apparent diffusion coefficient of water tracers, determined by several experimental methods and in bentonites containing 50 to 100% Na-montmorillonite, for $\rho_{b,mont}$ in the range 0.2 kg dm^{-3} (a dilute montmorillonite gel) to 1.5 kg dm^{-3} or more (compacted bentonite with ~80% of its pore volume located in montmorillonite interlayers).

CONCLUSIONS

The relative apparent diffusion coefficient (D_a/D_0) of water tracers in water-saturated bentonite is affected by both the geometry of the pore network and by the lower mobility of water molecules near the montmorillonite basal surfaces. The latter effect is negligible for the largest pores, but is very important for interlayer nanopores, in which all water molecules are in close proximity to montmorillonite basal surfaces. We have described this situation by conceptually dividing the pore space of compacted, water-saturated bentonite into macropore and interlayer nanopore compartments to develop a model of the diffusion of water tracers in Na-bentonite. In this model, the relative apparent diffusion coefficient is the weighted average of D_a/D_0 in the macropore and nanopore compartments, with weighting by their respective mole fractions of pore water. With a single fitted parameter, a geometric factor (G) equal to 4.0 ± 1.6, our model successfully describes all available experimental data on the mean principal relative apparent diffusion coefficient for water tracers in compacted, water-saturated bentonite. The model also yields a good description of the diffusion of water tracers in montmorillonite gels ($\rho_{b,mont} = 0.2$ to ~1.0 kg dm^{-3}), even though XRD experiments have not revealed the presence of interlayer nanopores at such low partial montmorillonite dry densities.

From comparison of our model to experimental data, the following trends can be inferred in the relation between D_a/D_0 and $\rho_{b,mont}$ for water tracers in water-saturated Na-bentonite. Between partial montmorillonite dry densities of 0 and 0.2 kg dm^{-3} (*i.e.* montmorillonite suspensions), the geometric factor increases rapidly with increasing $\rho_{b,mont}$, causing a fourfold decrease in D_a/D_0. Between partial montmorillonite dry densities of 0.2 and 1.72 kg dm^{-3} (dilute gel to highly compacted bentonite), the geometric factor is constant within experimental precision, while the constrictivity factor (δ) slowly decreases with $\rho_{b,mont}$, as an increasing fraction of the pore water becomes located in interlayer nanopores, eventually causing a further threefold decrease in D_a/D_0.

We confirm also that the relative apparent diffusion coefficient of water tracers is greater in the direction normal ($D_{a,\perp}$) *vs.* parallel to compaction ($D_{a,\parallel}$) in one-dimensionally-compacted bentonites. Thus predictions of the performance of isotropically-compacted bentonite in barriers require experimental determinations of the mean principal value of the apparent diffusion coefficient tensor. Overall we conclude that, in waste disposal situations, bentonite barriers formed by compacting dry bentonite powders in the direction of the expected contaminant transport may perform better than barriers prepared by isotropic compaction. However, the magnitude of compaction-induced anisotropy in the apparent diffusion coefficient tensor as a function of partial montmorillonite dry density and bentonite mineralogical composition should be investigated more thoroughly.

REFERENCES

Alonso, E. and Navarro, V. (2002) Modelling long term deformation of clay. Pp. 167–176 in: *Chemo-Mechanical Coupling in Clays* (C. Di Maio, T. Hueckel and B. Loret, editors). Balkema Publishers, Lisse, The Netherlands.

ANDRA (2001) *Reférentiel Matériaux, Tome 2, Les Minéraux Argileux*. Report C.RP.AMAT.01.060. ANDRA (Agence Nationale pour la Gestion des Déchets Radioactifs), Châtenay-Malabry, France.

Bear, J. (1972) *Dynamics of Fluids in Porous Media*. Dover Publications, New York.

Bérend, I., Cases, J.-M., François, M., Uriot, J.-P., Michot, L.J., Masion, A. and Thomas, F. (1995) Mechanism of adsorption and desorption of water vapor by homoionic montmorillonites. 2: The Li$^+$, Na$^+$, K$^+$, Rb$^+$ and Cs$^+$ exchanged forms. *Clays and Clay Minerals*, **43**, 324–336.

Bourg, I.C. (2004) Diffusion of water and inorganic ions in

saturated compacted bentonite. PhD thesis, University of California, Berkeley, 368 pp.

Boving, T.B. and Grathwohl, P. (2001) Tracer diffusion coefficients in sedimentary rocks: correlation to porosity and hydraulic conductivity. *Journal of Contaminant Hydrology*, **53**, 85−100.

Bradley, W.F. (1959) Density of water sorbed on montmorillonite. *Nature*, **183**, 1614−1615.

Calvet, R. (1973) Hydratation de la montmorillonite et diffusion des cations compensateurs. *Annales Agronomiques*, **24**, 77−217.

Cases, J.M., Bérend, I., Besson, G., François, M., Uriot, J.P., Thomas, F. and Poirier, J.E. (1992) Mechanism of adsorption and desorption of water vapor by homoionic montmorillonite: 1. The sodium exchanged form. *Langmuir*, **8**, 2730−2739.

Chang, F.-R.C., Skipper, N.T. and Sposito, G. (1995) Computer simulation of interlayer molecular structure in sodium montmorillonite hydrates. *Langmuir*, **11**, 2734−2741.

Chantong, A. and Massoth, F.E. (1983) Restrictive diffusion in aluminas. *American Institute of Chemical Engineers Journal*, **29**, 725−731.

Choi, J.-W. and Oscarson, D.W. (1996) Diffusive transport through compacted Na- and Ca-bentonite. *Journal of Contaminant Hydrology*, **22**, 189−202.

Crank, J. (1975) *The Mathematics of Diffusion*, 2nd edition. Clarendon Press, Oxford, UK, 414 pp.

Dykhuizen, R.C. and Casey, W.H. (1989) An analysis of solute diffusion in rocks. *Geochimica et Cosmochimica Acta*, **53**, 2793−2805.

Eriksen, T.E., Jansson, M. and Molera, M. (1999) Sorption effects on cation diffusion in compacted bentonite. *Engineering Geology*, **54**, 231−236.

Gay-Duchosal, M., Powell, D.H., Lechner, R.E. and Rufflé, B. (2000) QINS studies of water diffusion in Na-montmorillonite. *Physica B*, **276/278**, 234−235.

Grim, R.E. (1968) *Clay Mineralogy*, 2nd edition. McGraw-Hill, New York, 596 pp.

Güven, N. (1992) Rheological aspects of aqueous smectite suspensions. Pp. 81−126 in: *Clay-Water Interface and its Rheological Implications* (N. Güven and R.M. Pollastro, editors). The Clay Minerals Society, Boulder, CO.

Hall, P.L., Ross, D.K., Tuck, J.J. and Hayes, M.H.B. (1978) Dynamics of interlamellar water in divalent cation exchanged expanding lattice clays. Pp. 617−635 in: *Proceedings of the IAEA Symposium on Neutron Inelastic Scattering, Vienna 1977*, Vol. 1. International Atomic Energy Agency, Vienna.

Hueckel, T., Loret, B. and Gajo, A. (2002) Expansive clays as two-phase, deformable reactive continua: Concepts and modeling options. Pp. 105−120 in: *Chemo-Mechanical Coupling in Clays* (C. Di Maio, T. Hueckel and B. Loret, editors). Swets & Zeitlinger, Lisse, The Netherlands.

Ichikawa, Y., Kawamura, K., Fujii, N. and Kitayama, K. (2004) Microstructure and micro/macro-diffusion behavior of tritium in bentonite. *Applied Clay Science*, **26**, 75−90.

JNC (2000) *H12: Project to establish the scientific and technical basis for HLW disposal in Japan, supporting report 3: safety assessment of the geological disposal system*. JNC Technical Report TN1410 2000-04. Japan Nuclear Cycle Development Institute, 445 pp.

Kato, H., Muroi, M., Yamada, N., Ishida, H. and Sato, H. (1995) Estimation of effective diffusivity in compacted bentonite. Pp. 277−284 in: *Scientific Basis for Nuclear Waste Management XVIII* (T. Murakami and R.C. Ewing, editors). Materials Research Society, Pittsburgh, Pennsylvania.

Kemper, W.D., Maasland, D.E.L. and Porter, L. (1964)

Mobility of water adjacent to mineral surfaces. *Soil Science Society of America Proceedings*, **28**, 164−167.

Keren, R. and Shainberg, I. (1975) Water vapor isotherms and heat of immersion of Na/Ca-montmorillonite systems. I: Homoionic clays. *Clays and Clay Minerals*, **23**, 193−200.

Kozaki, T., Sato, H., Fujishima, A., Sato, S. and Ohashi, H. (1996) Activation energy for diffusion of cesium in compacted sodium montmorillonite. *Journal of Nuclear Science and Technology*, **33**, 522−524.

Kozaki, T., Sato, H., Fujishima, A., Saito, N., Sato, S. and Ohashi, H. (1997) Effect of dry density on activation energy for diffusion of strontium in compacted sodium montmorillonite. Pp. 893−900 in: *Scientific Basis for Nuclear Waste Management XX* (W.J. Gray and I.R. Triay, editors). Materials Research Society, Pittsburgh, Pennsylvania.

Kozaki, T., Fujishima, A., Sato, S. and Ohashi, H. (1998) Self-diffusion of sodium ions in compacted montmorillonite. *Nuclear Technology*, **121**, 63−69.

Kozaki, T., Sato, Y., Nakajima, M., Kato, H., Sato, S. and Ohashi, H. (1999) Effect of particle size on the diffusion behavior of some radionuclides in compacted bentonite. *Journal of Nuclear Materials*, **270**, 265−272.

Kozaki, T., Inada, K., Sato, S. and Ohashi, H. (2001a) Diffusion mechanism of chloride ions in sodium montmorillonite. *Journal of Contaminant Hydrology*, **47**, 159−170.

Kozaki, T., Suzuki, S., Kozai, N., Sato, S. and Ohashi, H. (2001b) Observation of microstructures of compacted bentonite by microfocus X-ray computerized tomography (Micro-CT). *Journal of Nuclear Science and Technology*, **38**, 697−699.

LaGrega, M.D., Buckingham, P.L. and Evans, J.C. (2001) *Hazardous Waste Management*, 2nd edition. McGraw-Hill, Boston.

Lehikoinen, J., Muurinen, A. and Valiainen, M. (1999) A consistent model for anion exclusion and surface diffusion. Pp. 663−670 in: *Scientific Basis for Nuclear Waste Management XXII* (D. Wronkiewicz and J. Lee, editors). Materials Research Society, Pittsburgh, Pennsylvania.

Liu, J., Yamada, H., Kozaki, T., Sato, S. and Ohashi, H. (2003a) Effect of silica sand on activation energy for diffusion of sodium ions in montmorillonite and silica sand mixture. *Journal of Contaminant Hydrology*, **61**, 85−93.

Liu, J., Kozaki, T., Horiuchi, Y. and Sato, S. (2003b) Microstructure of montmorillonite/silica sand mixture and its effects on the diffusion of strontium ions. *Applied Clay Science*, **23**, 89−95.

Low, P.F. and Anderson, D.M. (1958) The partial specific volume of water in bentonite suspensions. *Soil Science Society of America Proceedings*, **22**, 22−24.

Madsen, F.T. (1998) Clay mineralogical investigations related to nuclear waste disposal. *Clay Minerals*, **33**, 109−129.

Marry, V. and Turq, P. (2003) Microscopic simulations of interlayer structure and dynamics in bihydrated heteroionic montmorillonites. *Journal of Physical Chemistry B*, **207**, 1832−1839.

McCombie, C. (1997) Nuclear waste management worldwide. *Physics Today*, **50(6)**, 56−62.

Michot, L.J., Villiéras, F., François, M., Bihannic, I., Pelletier, M. and Cases, J.-M. (2002) Water organisation at the solid-aqueous solution interface. *Comptes Rendus Geoscience*, **334**, 611−631.

Mills, R. (1973) Self-diffusion in normal and heavy water in the range 1-45°. *Journal of Physical Chemistry*, **77**, 685−688.

Molera, M. and Eriksen, T.E. (2002) Diffusion of $^{22}Na^+$, $^{85}Sr^{2+}$, $^{134}Cs^+$ and $^{57}Co^+$ in bentonite clay compacted to different densities: experiments and modeling. *Radiochimica Acta*, **90**, 753−760.

Murad, M.A. and Cushman, J.H. (2000) Thermomechanical

theories for swelling porous media with microstructure. *International Journal of Engineering Science*, **38**, 517−564.

Muurinen, A., Penttilä-Hiltunen, P. and Rantanen, J. (1987) Diffusion mechanisms of strontium and cesium in compacted sodium bentonite. Pp. 803−812 in: *Scientific Basis for Nuclear Waste Management X* (J.K. Bates and W.B. Seedfeldt, editors). Materials Research Society, Pittsburgh, Pennsylvania.

Muurinen, A., Penttilä-Hiltunen, P. and Uusheimo, K. (1989) Diffusion of chloride and uranium in compacted sodium bentonite. Pp. 743−748 in: *Scientific Basis for Nuclear Waste Management XII* (W. Lutze and R.C. Ewing, editors). Materials Research Society, Pittsburgh, Pennsylvania.

Nakashima, Y. (2000) Pulsed field gradient proton NMR study of the self-diffusion of H_2O in montmorillonite gel: Effects of temperature and water fraction. *American Mineralogist*, **85**, 132−138.

Nakashima, Y. (2002) Diffusion of H_2O and I^- in expandable mica and montmorillonite gels: contribution of bound H_2O. *Clays and Clay Minerals*, **50**, 1−10.

Nakashima, Y. (2004) Nuclear magnetic resonance properties of water-rich gels of Kunigel-V1 bentonite. *Journal of Nuclear Science and Technology*, **41**, 981−992.

Nakazawa, T., Takano, M., Nobuhara, A., Torikai, Y., Sato, S. and Ohashi, H. (1999) Activation energies of diffusion of tritium and electrical conduction in water-saturated compacted sodium montmorillonite. In: *Radioactive Waste Management and Environmental Remediation*, American Society of Mechanical Engineers, 5 pp.

Ochs, M., Lothenbach, B., Wanner, H., Sato, H. and Yui, M. (2001) An integrated sorption-diffusion model for the calculation of consistent distribution and diffusion coefficients in compacted bentonite. *Journal of Contaminant Hydrology*, **47**, 283−296.

Pezerat, H. and Méring, J. (1967) Recherches sur la position des cations échangeables et de l'eau dans les montmorillonites. *Comptes Rendus de l'Académie des Sciences de Paris, Série D*, **265**, 529−532.

Pusch, R. (1999) Microstructural evolution of buffers. *Engineering Geology*, **54**, 33−41.

Sato, H. and Suzuki, S. (2003) Fundamental study on the effect of an orientation of clay particles on diffusion pathways in compacted bentonite. *Applied Clay Science*, **23**, 51−60.

Sato, H., Ashida, T., Kohara, Y., Yui, M. and Sasaki, N. (1992) Effect of dry density on diffusion of some radionuclides in compacted sodium bentonite. *Journal of Nuclear Science and Technology*, **29**, 873−882.

Satterfield, C.N., Colton, C.K. and Pitcher, W.H., Jr. (1973) Restricted diffusion in liquids with fine pores. *American Institute of Chemical Engineers Journal*, **19**, 628−635.

Shackelford, C.D. (1991) Laboratory diffusion testing for waste disposal − A review. *Journal of Contaminant Hydrology*, **7**, 177−217.

Shackelford, C.D. and Lee, J.-M. (2003) The destructive role of diffusion on clay membrane behavior. *Clays and Clay Minerals*, **51**, 186−196.

Sposito, G. (1992) The diffuse-ion swarm near smectite particles suspended in 1:1 electrolyte solutions: modified Gouy-Chapman theory and quasicrystal formation. Pp. 128−155 in: *Clay-Water Interface and its Rheological Implications* (N. Güven and R.M. Pollastro, editors). The Clay Minerals Society, Boulder, CO.

Sposito, G., Gupta, V.K. and Bhattacharya, R.N. (1979) Foundation theories of solute transport in porous media: a critical review. *Advances in Water Resources*, **2**, 59−68.

Suzuki, S., Sato, H., Ishidera, T. and Fujii, N. (2004) Study on anisotropy of effective diffusion coefficient and activation energy for deuterated water in compacted sodium bentonite. *Journal of Contaminant Hydrology*, **68**, 23−37.

Torstenfelt, B. (1986) Migration of the fission products strontium, technetium, iodine and cesium in clay. *Radiochimica Acta*, **39**, 97−104.

van Brakel, J. and Heertjes, P.M. (1974) Analysis of diffusion in macroporous media in terms of a porosity, a tortuosity and a constrictivity factor. *International Journal of Heat and Mass Transfer*, **17**, 1093−1103.

van Schaik, J.C., Kemper, W.D. and Olsen, S.R. (1966) Contribution of adsorbed cations to diffusion in clay-water systems. *Soil Science Society of America Proceedings*, **30**, 17−22.

Watanabe, T. and Sato, T. (1988) Expansion characteristics of montmorillonite and saponite under various relative humidity conditions. *Clay Science*, **7**, 129−138.

Zheng, C. and Bennett, G.D. (1995) *Applied Contaminant Transport Modelling: Theory and Practice*. Van Nostrand Reinhold, New York.